

Thermal conductivity of solid hydrogen with ortho-hydrogen concentrations between 20 and 70 at. %

J. E. Huebler* and R. G. Bohn

Department of Physics and Astronomy, The University of Toledo, Toledo, Ohio 43606

(Received 5 August 1977)

We have measured the thermal conductivity of solid hydrogen in the temperature range of 1.4–13 K. Measurements were taken on a single sample over a 196-h period. During this time the ortho-hydrogen concentration changed from 75 to 19.8 at.%. Because precise temperature control allowed corrections to be made for changing ortho concentration, thermal conductivity versus temperature is given for constant ortho-hydrogen concentrations of 20, 30, 40, 50, 60, and 70 at.%. Addition of thermal resistances was assumed and several curve fits to the data are given, including one with terms proportional to $c^2 T^{-2}$ and cT^{-3} . An umklapp term is given that also agrees well with the data from previous experiments.

I. INTRODUCTION

The first measurements of thermal conduction in solid hydrogen were done by Hill and Schneidmesser¹ for ortho-hydrogen (*o*-H₂) concentrations ranging from 0.5% to 72% over a temperature range from 2 to 12 K. They deduced that the thermal resistance that could be attributed to the *o*-H₂ molecules had a temperature dependence that varied as T^{-n} , where $2 < n < 3$. Subsequent measurements by Bohn and Mate,² and Constable and Gaines³ have concentrated on para-hydrogen (*p*-H₂) (or HD in the case of Constable and Gaines) with small concentrations of *o*-H₂ molecules, $c \leq 0.05$. At low concentrations of *o*-H₂, the effect of isolated *o*-H₂ molecules on the thermal resistance could be determined more readily. A theoretical paper by Ebner and Sung⁴ looked at this effect specifically and predicted a $c^2 T^{-2}$ dependence for the resistance at low temperatures and low concentrations. This was only in qualitative agreement with Bohn and Mate, who obtained a cT^{-3} dependence. The measurements by Constable and Gaines at temperatures less than 1 K, however, confirmed the results by Ebner and Sung. In 1975 Kokshenev⁵ took the effect of *o*-H₂ pairs into account and obtained results that were in better agreement with Bohn and Mate, although difficulties arise for $c \geq 0.05$ because of the effect of higher-order clusters.

The purpose of the present work is to extend the measurements of Hill and Schneidmesser to include a greater temperature range and to improve the overall accuracy. In addition, we have made use of the fact that the *o*-H₂ concentration in solid hydrogen is time dependent.⁶ A single sample was grown at the beginning of the experiment, and measurements were performed over a period of approximately 200 h. This method allowed us to remove any variation that might occur if a new

crystal were grown for each concentration. In addition, the changes in *o*-H₂ concentration could be explicitly taken into account. Since normal processes are extremely rapid in solid hydrogen³ ($\tau_N \rightarrow 0$), the additive resistive approximation would appear to be valid. Using this approximation, we hope to determine explicit expressions for the umklapp resistance, impurity resistance, boundary resistance, and the resistance due to the presence of *o*-H₂ molecules.

II. EXPERIMENTAL

Figure 1 is a schematic drawing of the lower portion of the cryostat which includes the cell into which the H₂ was condensed and solidified. This cell was made of stainless steel (0.952-cm diameter, 0.018-cm wall thickness, 5.0-cm height) which was soft soldered to a copper base. The top of the cell was also copper and had a germanium resistance thermometer and an evanohm heater ($R_C = 987.5 \Omega$) mounted on it. The resistance thermometer had been calibrated with a standard traceable to the National Bureau of Standards Provisional Scale of 1965. This calibration was checked periodically during the course of the experiments and found to be accurate to within 0.005 K from 1.5 to 20 K. Special care was taken to insure that the electrical leads were thermally anchored at the cell top as well as at other positions in the cryostat.

Since the two-heater method as described by Bohn and Mate² was to be used for the measurements, copper fins spaced 1.137 cm apart were mounted in slots cut in the stainless-steel cell. Evanohm heaters ($R_A = 981.7 \Omega$, $R_B = 982.1 \Omega$) were then wound on these fins. A radiation shield (not shown) surrounded the sample cell.

A temperature controller, based on a design by Tominaga,⁷ was used to control the tempera-

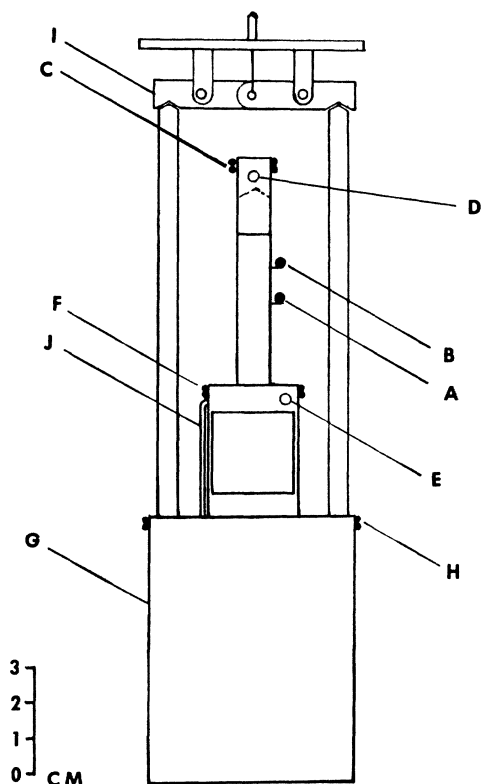


FIG. 1. Cryostat schematic. *A*—sample heater H_A ; *B*—sample heater H_B ; *C*—sample heater H_C ; *D*—sample thermometer; *E*—thermometer for temperature controller; *F*—heater for temperature controller; *G*—helium reservoir; *H*—helium reservoir heater; *I*—mechanical heat switch; *J*—hydrogen fill line.

ture of the sample-cell base. The temperature controller sensing element was mounted in the sample base along with a germanium resistance thermometer that had been calibrated previously between 1.21 and 4.2 K.⁸ This calibration was extended to 17 K by calibrating it against the germanium thermometer at the top of the sample cell. Where they overlap, the two calibrations agree. By recording temperature as a function of time, it was estimated that the stability of the sample cell base $\Delta T/T$ was approximately 0.1% at 1 K.

The rest of the cryostat is of a somewhat conventional design. The helium reservoir was filled through a needle valve with liquid helium from the ⁴He Dewar when the measurements below 4.2 K were taken. Above 4.2 K, a combination of the ⁴He exchange gas in the reservoir, a mechanical heat switch, and electrical heaters allowed us to maintain a temperature anywhere between 4.2 and 20 K.

A four-wired dc method was used to measure

the resistance of the two germanium resistance thermometers. By using a Leeds and Northrup K-5 potentiometer, a Keithley 147 nanovolt null detector, and a Keithley 225 constant current source, a precision of one part in 10^5 was attainable in the resistance measurement at 1.5 K. A potentiometric method was also used to measure the dc power inputs to the sample-cell heaters since the two-heater method of measurement requires that the power inputs are the same.

The majority of the data were taken in a single continuous experiment lasting 196.5 h. Data from previous experiments had been collected for solid hydrogen as well as for the stainless-steel sample cell. The hydrogen data from two different experiments agreed to within the experimental error.

Hydrogen gas⁹ which had a purity of 99.995% was condensed into the cryostat at its saturated vapor pressure from a room-temperature gas-handling system. By monitoring the amount of hydrogen remaining at room temperature, it was possible to determine when the lower part of the fill line and cell were filled with liquid. This process took approximately 45 min. The temperature of the cell base was then lowered and the solid-liquid phase boundary was allowed to move up the sample cell at a rate that was determined by the power input to the heaters. The solidification process was completed within about 2 h. The crystal was grown rather slowly to minimize the number of physical imperfections and to insure good thermal contact with the heaters and sample cell base. By using the heaters H_A , H_B , and occasionally the heater at the top of the sample cell individually, a one-heater, one-thermometer method (see Appendix) could be used to determine the thermal conductivity between the cell base and the cell top. The data obtained from this method were consistent with that obtained from the two-heater method. Thus, it would appear that the crystal quality was the same over the whole length of the sample. No special annealing was attempted because of our desire to obtain data for *o*-H₂ concentrations near 75%. The first data point was taken 5 h after one-half of the hydrogen had been condensed ($t=0$). The first set of data consisted of measurements above 4 K. Low- (1.5–4.2 K) and high- (4.2–12 K) temperature data were then taken on alternate days. A series of temperatures that spanned the appropriate temperature range were chosen and data were collected at these selected temperatures only. The two-heater method (with temperature differences of ~ 0.1 K) was the primary source of the data. This technique was checked for each measurement with the one-heater method. The

time at which each data point was taken was also recorded.

The conductivity was then determined and corrected for the stainless-steel sample cell. These data are shown in Fig. 2. Since each point was taken at a different time (hence, a different concentration), the curves do not represent the conductivity at constant concentration. Using Schmidt's value for the rate constant [$\eta = 19.0 \times 10^{-5}$ (% h⁻¹)], the concentration for each data point was determined. (Although this value for the rate constant differs somewhat from that given by Ahlers,¹⁰ we feel that the resulting uncertainty in the concentration is less than 4% and is a result of the uncertainty in the rate constant.) One could then choose those data points that were taken at one of the previously selected temperatures, and make isothermal plots of conductivity versus concentration. In particular, a logarithmic plot yielded a series of straight lines for temperatures less than 7.2 K. The conductivity at constant *o*-H₂ concentration could then be de-

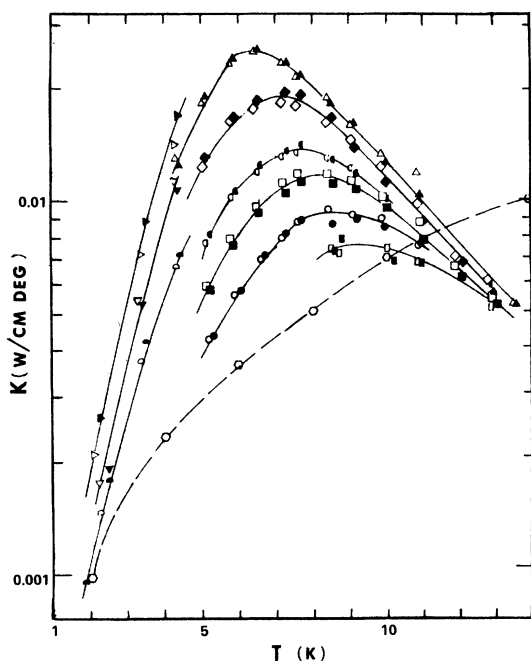


FIG. 2. Original thermal-conductivity data vs temperature. Each symbol represents a sequence of measurements. The open symbols are for the one-heater method and the solid symbols are for the two-heater method. Since the *o*-H₂ concentration is time dependent, each point in a sequence is at a different concentration. The dashed line is for the stainless steel of the sample cell. The range of *o*-H₂ concentrations for each sequence is: \triangleright : 19.8%–20.4%; \triangle : 21.7%–22.5%; ∇ : 23.9%–24.5%; \diamond : 26.9%–28.2%; \triangleleft : 30.6%–35.7%; \square : 36.2%–37.9%; \square : 41.8%–45.2%; \circ : 51.0%–57.2%; \square : 64.8%–70.0%.

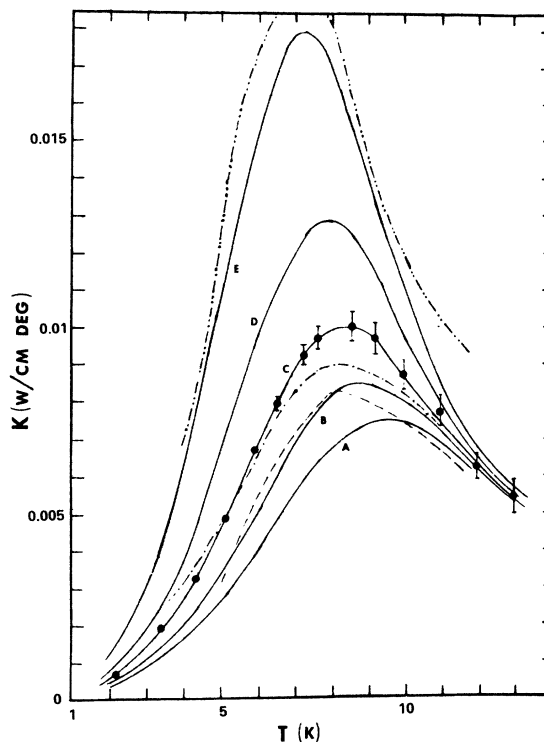


FIG. 3. Thermal conductivity of hydrogen at constant *o*-H₂ concentration vs temperature. The temperatures that were used to obtain these curves are indicated by the solid circles. The figure also includes error estimates and some of Hill and Schneidmesser's results (Ref. 1). A: 70%; B: 60%; C: 50%; D: 40%; E: 30% (this paper). From Ref. 1: - · - · 29%; - · - · 55%; - - - 72%.

termined. It should be mentioned that the low-temperature-high-concentration portion of the curves in Fig. 3 required an extrapolation rather than an interpolation of the data. While there is a danger in doing this, a similar extrapolation for data points at higher temperatures ($T < 7$ K) produced agreement with data that were obtained for $c \geq 0.50$.

Estimates of the relative error were made. These range from 2.4% at 1.5 K to 11% at 13 K and are indicated in Fig. 3. The major source of error for increasing temperatures was the decreasing sensitivity of the carbon resistance thermometer used in the temperature controller.

III. RESULTS AND DISCUSSION

Thermal conductivity is plotted versus temperature for several ortho-hydrogen concentrations in Fig. 3. It can be seen that the conductivity increases as the ortho-hydrogen concentration decreases. This is also the general trend obtained in previous measurements.¹⁻³

Generally, one would assume that the total thermal resistance could be written in the form (all thermal resistances will be in units of cm K/W)

$$W = pT^{-3} + bT^{1.5} + dT^n e^{-\Theta/\beta T} + W_{\text{ortho}}. \quad (1)$$

The terms, considered in reverse order, are due to the presence of *o*-H₂ molecules, phonon scattering by umklapp processes, scattering by point defects (if any), and boundary scattering. For classical boundary scattering in a single crystal, *p* is determined by the size of the crystal. If this is true in our case, the *T*⁻³ term would make a very small contribution to the total thermal resistance (diameter of sample ~1 cm). However, if *p* were determined by the size of a crystallite, then it is conceivable that there would be an effect on the thermal resistance. During the course of the curve fitting procedures it was determined that a constant value for *p* would *not* give a good fit to the data and that this was independent of the form of *W*_{ortho}. In addition, letting *p* vary and setting *W*_{ortho} = 0 did not give a good fit to the data. Thus, we feel that the effects of normal boundary scattering are small and are being masked by the term *W*_{ortho}.

Several forms for *W*_{ortho} were chosen and attempts were made to fit the data. Although some were rejected on the basis of chi-square tests, others described the data equally well (within the experimental error), so that there resulted no *unique* fit.

For instance, if *c* is the *o*-H₂ concentration, one can use the form

$$W_{\text{ortho}} = rc^m T^{-n} \quad (2)$$

in Eq. (1) with *b* = 0. The values of the parameters would be

$$r = 2.88 \times 10^4, \quad m = 1.60, \quad n = 2.35,$$

$$d = 6.25 \times 10^6, \quad \Theta/\beta = 59.7,$$

and this could provide a reasonable description of the data (reduced chi-square = $\chi^2_{\nu} \sim 1$).¹¹ Although this form for *W*_{ortho} is perhaps the simplest, the physical justification for its use is not apparent since there is at present no theory to describe the conduction process in solid hydrogen with high *o*-H₂ concentrations.

The value for *n* in the above suggests that another form for *W*_{ortho} might be

$$W_{\text{ortho}} = g_i T^{-2} + h_i T^{-3}, \quad (3)$$

where *g*_{*i*} and *h*_{*i*} are to be determined for each *o*-H₂ concentration. During the preliminary fitting procedures it was discovered that *g*_{*i*} ∝ *c*² and that *h*_{*i*} ∝ *c* to within the experimental error. Thus, the

total thermal resistance could be written

$$W_T = hcT^{-3} + gc^2 T^{-2} + bT^{1.5} + dT^{-f} e^{(-59.17/T)}, \quad (4)$$

where *h*, *g*, *b*, *d*, and *f* are to be determined. The values obtained from the fitting program are, *h* = 16593, *g* = 13900, *b* = 0.35, *d* = 1.64 × 10⁶, and *f* = 1.87. Let us consider each term in the above equation in reverse order. The umklapp term was chosen with $\Theta/\beta = 59.17$ K. A simple isotropic model¹² for umklapp processes predicts a maximum value for β of 2. However, this does not take such things as anisotropy and dispersion into account and one finds that in practice β may be less than or greater than 2.¹³ If we assume that $\beta = 2$, then $\Theta = 118$ K, which is within the range of Debye temperatures obtained from specific-heat measurements.¹⁴⁻¹⁶ The value of *f* is usually about 2 or 3 and the value obtained from the fitting procedures agrees reasonably well. The value for *d* depends on the crystal structure and the specific model for the interatomic forces.

An attempt was made to compare the umklapp term in Eq. (4) to that obtained in other experiments.^{1,2,17} A different fitting procedure was tried in which an attempt was made to separate the umklapp resistance from the other terms in the thermal resistance. The umklapp resistance that we obtained was

$$W_u = 2.49 \times 10^6 T^{-2} e^{(-59.7/T)}, \quad (5)$$

and the results are shown in Fig. 4. This figure also shows the umklapp term obtained from Eq. (4). Systematic differences between the data from different experiments might be expected since the thermal conductivity in the umklapp region is anisotropic.¹³ Thus, Eq. (5) is descriptive of the data in general, but additional data is required to specifically relate *W*_{*u*} to crystallographic orientation.

The point defect term has a coefficient of 0.35. This corresponds to an impurity concentration of approximately 0.2% if the impurities are D₂ or 0.005% if they are N₂ impurities. This can be compared to the 0.005% impurity concentration claimed by the gas supplier. One should also note that impurity concentrations determined by thermal-conductivity measurements are often an order of magnitude higher than those obtained by mass spectrograph analysis.

The second term *gc*²*T*⁻² is the same form as that proposed by Ebner and Sung.⁴ The coefficient *g* in Ebner and Sung's theory is related to the parameter ϵ^2 . Now the interaction responsible for the phonon-*o*-H₂ scattering is the difference of interactions between a *p*-H₂+*p*-H₂ pair and a *p*-H₂+*o*-H₂ pair. The strength and form of this interaction has not been accurately determined,

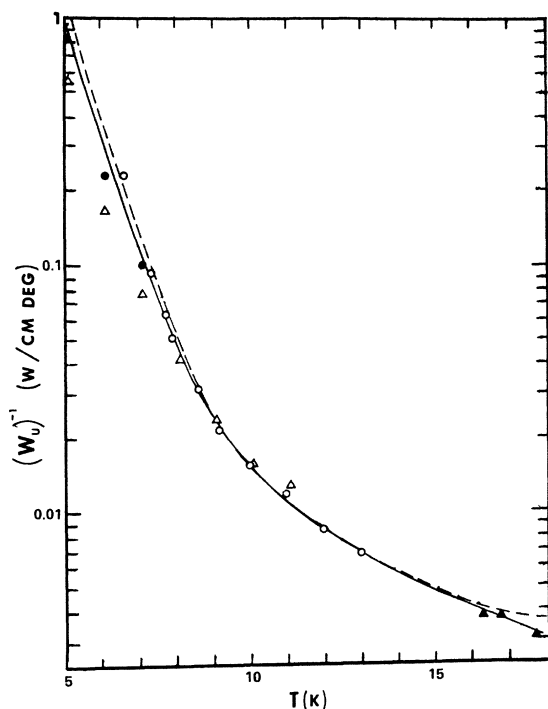


FIG. 4. Reciprocal of umklapp resistance vs temperature. \circ , Data (this paper); \bullet , Bohn and Mate (H_2) (Ref. 2); \triangle , Hill and Schneidmesser (H_2) (Ref. 1); \blacktriangle , Daney (D_2) (Ref. 17); —, $W_u = 2.49 \times 10^6 T^{-2} e^{-59.7/T}$; ---, $W_u = 1.64 \times 10^6 T^{-1.87} e^{-53.2/T}$.

but is usually given as an exponential-6 model modified by the angular dependence of the hydrogen molecules under consideration.^{4,18,19} Van Kranendonk and Sears¹⁸ use the form

$$H_{o-p} \propto [V e^{[-\eta(R-a)/a]} - \epsilon(a/R)^6] Y_{20}(\omega), \quad (6)$$

where a is the nearest-neighbor distance, V and ϵ are the strengths of the anisotropic overlap and dispersion forces, respectively, η gives the range of the overlap forces, and ω describes the orientation of the $o\text{-H}_2$ molecule with respect to the intermolecular axis. The values of V , η , and ϵ are not well known. In addition, Eq. (6) is for a static crystal. The interaction must be suitably averaged over the zero-point motions of hydrogen. This average does not change the form of Eq. (6), but it does give effective values for the coefficients, in particular $\bar{\epsilon}$ for ϵ . Thus, $\bar{\epsilon}$, and therefore $\bar{\epsilon}^2$, are directly related to the difference in interactions between $p\text{-H}_2 + p\text{-H}_2$ and $p\text{-H}_2 + o\text{-H}_2$. In practice \bar{V} , $\bar{\eta}$, and $\bar{\epsilon}$ are fit to the data under consideration.

The coefficient of our $c^2 T^{-2}$ term, $1.39 \times 10^4 \text{ K}^3 \text{ cm/W}$ compares to the value of $2.7 \times 10^4 \text{ K}^3 \text{ cm/W}$ that Ebner and Sung used to fit Bohr and Mate's data. The value of $2.7 \times 10^4 \text{ K}^3 \text{ cm/W}$ is approxi-

mately three times larger than the value predicted by Ebner and Sung's theory. Constable and Gaines³ obtained a coefficient of $1.82 \times 10^5 \text{ K}^3 \text{ cm/W}$. Thus our value of $1.39 \times 10^4 \text{ K}^3 \text{ cm/W}$ is closest to Ebner and Sung's theory. This may be only a coincidence. Their theory is for concentrations smaller than 10% $o\text{-H}_2$, while our measurements were at a concentration of 20% or greater. It should be reemphasized that Ebner and Sung's prediction of $W \propto c^2 T^{-2}$ does not fit Bohn and Mate's data well.

The coefficient of the cT^{-3} term, 1.66×10^4 , is large compared to that of Bohn and Mate. Since this becomes the dominant term as one goes to lower temperatures (below the thermal-conductivity peak), it might be expected that an extrapolation of these results to lower concentrations would disagree with those of Bohn and Mate. This does occur, with the extrapolation of the conductivity being a factor 2–5 less than the data obtained for concentrations of $c \leq 0.05$. [A similar difficulty exists with the data of Hill and Schneidmesser,¹ but here one cannot extrapolate their own high-concentration data ($c \geq 0.05$) and obtain the conductivity of their $c = 0.005$ curve.] Clearly, however, one must be careful here since a true comparison should be made at low temperatures, away from the thermal-conductivity peak. Since the peak occurs at about 3 K for $c \sim 0.005$, additional data are needed (at all concentrations) at lower temperatures ($T < 2 \text{ K}$).

Recognizing that the low-concentration data² ($c \leq 0.05$) and the higher-concentration data were obtained under different experimental conditions, one might offer a possible explanation for this inconsistency. In their work on solid ^4He , Lawson and Fairbank¹³ observed that the umklapp term was anisotropic and noted that the thermal-conductivity peak was extremely sensitive to impurities. A similar situation might exist for hydrogen with the $o\text{-H}_2$ molecules acting as impurities. A rather dramatic suppression of the peak might occur as the $o\text{-H}_2$ concentration increased. Since the low-temperature side of the conductivity peak is apparently not governed by boundary scattering (as in the case for ^4He), one would not expect the curves for different $o\text{-H}_2$ concentrations to approach a common asymptote at low temperatures.

One might also argue that the failure of our results to extrapolate to the lower-concentration results might be due to a multicrystalline sample. To test this, the term hcT^{-3} was replaced in Eq. (4) by $(A + hc)T^{-3}$, where AT^{-3} is a standard boundary-scattering term. However, no value of A was found that improved the fit, so the original hcT^{-3} term was kept.

One cannot compare these results to calculations

for thermal conduction in solid hydrogen for $c > 0.1$. However, calculations have been made for the interactions of a phonon field and isolated singles and pairs of o -H₂ molecules ($c \sim 0.05$).^{4,5} In order to extend this to higher concentrations, one would have to include triangles of o -H₂ molecules as well as higher-order clusters. Miyagi²⁰ has calculated the energy levels of triangular clusters of o -H₂ molecules due to the electric quadrupole-quadrupole (EQQ) interaction for a rigid lattice. For each geometrical arrangement of the three molecules, there can be 27 energy levels. The interaction of the phonon field with these (and other) energy levels is obviously a complex problem but hopefully additional model calculations will be forthcoming.

Thus, while there is no really unique fit to the data, at least one fit is suggestive of some of the processes taking place in thermal conduction. Until an appropriate model or theory is advanced to describe these processes, it is difficult to choose one fit over another. In the future we expect to extend these measurements to lower temperatures and the other hydrogen modifications. We also hope to reconsider the Bohn and Mate data in terms of the techniques used in this paper.

The authors would like to thank the Research Corporation for their support during this work and Dr. John Johnson for his assistance with the computer program.

APPENDIX

In order to discuss the one-heater method let us assume that the crystal is in good thermal contact with the base and that the base is a heat sink of constant temperature T_0 . Turn on heater H_C with power \dot{Q}_1 . After a steady state is reached

the thermometer at the top of the sample cell T_R is at temperature T_1 and one can write

$$\dot{Q}_1 = K_1 A (T_1 - T_0) / l,$$

where A is the cross-sectional area of the crystal, and l is the length from the base to the heater. Now increase the power in heater H_C to \dot{Q}_2 and wait for steady-state conditions. If the new temperature of T_R is T_2 , we can write

$$\dot{Q}_2 = K_2 A (T_2 - T_0) / l.$$

If we assume that $T_2 - T_1$ is small enough so that $K_1 = K_2 = K$, we can subtract the equations to obtain

$$\dot{Q}_2 - \dot{Q}_1 = (KA/l)(T_2 - T_1).$$

Solving for K gives

$$K = (l/A)(\dot{Q}_2 - \dot{Q}_1) / (T_2 - T_1).$$

This method (like the two-heater method) has the advantage of requiring only one thermometer, plus the additional advantage of needing only one heater. Again any heat generated in the sample and any effects due to the geometry of the heater placement are subtracted out. The major disadvantage of this method is that it requires good thermal contact of the crystal with the base. If there is thermal-contact resistance at this point it will cause the conductivity to appear smaller than it is. If there is good contact with the base the two-heater method is, in effect, two one-heater methods (with $\dot{Q}_1 = 0$). If contact is not good, the combination of the two methods will give the contact resistance. For all the measurements presented in this paper, the thermal contact of the crystal with the base was good as there was no noticeable difference between the thermal conductivities obtained using the two methods.

*Present address: Institute of Gas Technology, Chicago, Ill. 60616.

¹R. W. Hill and B. Schneidmesser, *Z. Phys. Chem. Neue Folge* **16**, 257 (1958).

²R. G. Bohn and C. F. Mate, *Phys. Rev. B* **2**, 2121 (1970).

³J. H. Constable and J. R. Gaines, *Phys. Rev. B* **8**, 3966 (1973).

⁴C. Ebner and C. C. Sung, *Phys. Rev. B* **2**, 2115 (1970).

⁵V. B. Kokshenev, *J. Low Temp. Phys.* **20**, 373 (1975).

⁶F. Schmidt, *Phys. Rev. B* **10**, 4480 (1974).

⁷A. Tominaga, *Cryogenics* **11**, 389 (1971).

⁸R. G. Bohn, *J. Appl. Phys.* **45**, 2133 (1974).

⁹Matheson Gas Products, East Rutherford, N.J. 07073.

¹⁰G. Ahlers, *J. Chem. Phys.* **40**, 3123 (1964).

¹¹P. R. Bevington, *Data Reduction and Error Analysis*

for the Physical Sciences (McGraw-Hill, New York, 1969).

¹²J. M. Ziman, *Electrons and Phonons* (Clarendon, Oxford, 1967).

¹³D. T. Lawson and H. A. Fairbank, *J. Low Temp. Phys.* **11**, 363 (1973).

¹⁴R. W. Hill and O. V. Lounasmaa, *Philos. Mag.* **4**, 786 (1959).

¹⁵G. Ahlers, *J. Chem. Phys.* **41**, 86 (1964).

¹⁶R. J. Roberts and J. G. Daunt, *J. Low Temp. Phys.* **6**, 97 (1972).

¹⁷D. E. Daney, *Cryogenics* **11**, 290 (1971).

¹⁸J. Van Kranendonk and V. F. Sears, *Can. J. Phys.* **44**, 313 (1966).

¹⁹T. Nakamura, *Prog. Theor. Phys.* **14**, 135 (1955).

²⁰H. Miyagi, *Prog. Theor. Phys.* **40**, 1448 (1968).